Atmos. Meas. Tech., 9, 2055–2065, 2016
www.atmos-meas-tech.net/9/2055/2016/
doi:10.5194/amt-9-2055-2016

Atmospheric Measurement Techniques
Open Access
EGU

The impact of the ozone effective temperature on satellite validation using the Dobson spectrophotometer network

Maria Elissavet Koukouli[1], Marina Zara[1,3], Christophe Lerot[2], Konstantinos Fragkos[1], Dimitris Balis[1], Michel van Roozendael[2], Marcus Antonius Franciscus Allart[3], and Ronald Johannes van der A[3]

[1]Laboratory of Atmospheric Physics, Aristotle University of Thessaloniki, Thessaloniki, Greece
[2]Belgian Institute for Space Aeronomy (BIRA-IASB), Brussels, Belgium
[3]Koninklijk Nederlands Meteorologisch Instituut (KNMI), De Bilt, the Netherlands

Correspondence to: Maria Elissavet Koukouli (mariliza@auth.gr)

Received: 9 November 2015 – Published in Atmos. Meas. Tech. Discuss.: 14 January 2016
Revised: 19 April 2016 – Accepted: 21 April 2016 – Published: 9 May 2016

Abstract. The main aim of the paper is to demonstrate an approach for post-processing of the Dobson spectrophotometers' total ozone columns (TOCs) in order to compensate for their known stratospheric effective temperature (T_{eff}) dependency and its resulting effect on the usage of the Dobson TOCs for satellite TOCs' validation. The Dobson observations employed are those routinely submitted to the World Ozone and Ultraviolet Data Centre (WOUDC) of the World Meteorological Organization, whereas the effective temperatures have been extracted from two sources: the European Space Agency, ESA, Ozone Climate Change Initiative, Ozone-CCI, GODFIT version 3 (GOME-type Direct FITting) algorithm applied to the GOME2/MetopA, GOME2A, observations as well as the one derived from the European Centre for Medium-Range Weather Forecasts (ECMWF) outputs. Both temperature sources are evaluated utilizing co-located ozonesonde measurements also retrieved from the WOUDC database. Both GODFIT_v3 and ECMWF T_{eff}s are found to be unbiased against the ozonesonde observations and to agree with high correlation coefficients, especially for latitudes characterized by high seasonal variability in T_{eff}.

The validation analysis shows that, when applying the GODFIT_v3 effective temperatures in order to post-process the Dobson TOC, the mean difference between Dobson and GOME2A GODFIT_v3 TOCs moves from 0.63 ± 0.66 to 0.26 ± 0.46 % in the Northern Hemisphere and from 1.25 ± 1.20 to 0.80 ± 0.71 % in the Southern Hemisphere. The existing solar zenith angle dependency of the differences has been smoothed out, with near-zero dependency up to the 60–65° bin and the highest deviation decreasing from 2.38 ± 6.6 to 1.37 ± 6.4 % for the 80–85° bin. We conclude that the global-scale validation of satellite TOCs against collocated Dobson measurements benefits from a post-correction using suitably estimated T_{eff}s.

1 Introduction

Satellite observations of the total ozone column (hereafter, TOC) on a global scale have routinely been performed since the early 1970s and in the later years even concurrently by multiple instruments on different polar platforms such as the TOMS/EP, GOME/ERS-2, SCIAMACHY/Envisat, OMI/Aura and the recent OMPS/Suomi NPP, among others. The validation of these measurements using ground-based instrumentation as "truth" has also been an integral part of the satellite TOC time series production. Since years 1957/1958, also known as the International Geophysical Year, when the need for routine global TOC measurements was clearly demonstrated (Brönnimann et al., 2003), the first worldwide network of manually operated Dobson spectrophotometers was established. Later on, in the early 1980s, the fully automated Brewer spectrophotometer was launched and the global monitoring of the atmospheric ozone content was thus enhanced. Innumerous satellite validation studies have used these ground-based observations in order to assess the behaviour and accuracy of both their measurements and algorithm (for e.g. Lambert et al., 1999, 2000; Fioletov et al., 1999; Bramstedt et al., 2003; Weber et al., 2005; Balis et al., 2007a; among others). As satellite instrumentation

technology advanced and the associated retrieval algorithms became more sophisticated, the unavoidable shortcomings of the ground-based measurements became more of an issue than before. One such concern is the fact that the operational Dobson algorithm does not account for the natural intra-annual variability of the stratospheric temperature which in turn heavily affects the ozone absorption coefficients used in the Dobson TOC retrieval. However, as was discussed in Fioletov (2008), even during a simple day the tropopause height may alter significantly and bring changes in the TOC of up to 70 DU, which in turn could influence the ozone effective temperature. The Dobson algorithmic shortcomings may hence result in daily, seasonal or even interannual ozone column dependencies being introduced which unavoidably hinders the real performance of satellite total ozone algorithms when validated with Dobson measurements.

In this paper we shall introduce a post-processing of the daily TOC values formally reported to the World Meteorological Organization (WMO) World Ozone and Ultraviolet Data Centre (WOUDC) database. Effective temperatures, i.e the weighting of the atmospheric temperature profile with the ozone profile, hereafter T_{eff}, from both an algorithm and a model shall be utilized. The algorithm employed is the GOME2/MetopA European Space Agency, ESA, Climate Change Initiative project, Ozone-CCI, GODFIT (GOME-type Direct FITting) version 3 algorithm (Lerot et al., 2014), whereas the model results originate from the European Centre for Medium-Range Weather Forecasts (ECMWF) repository at http://www.ecmwf.int. As part of the ESA Ozone_cci project, the GODFIT_v3 algorithm has been applied among others to the GOME2/MetopA (hereafter GOME2A) observations, and the global validation of the GOME2A TOCs between 2007 and 2014 shall be used as an example for the possibilities of this type of post-processing improvement.

In Sect. 2.1 the Dobson spectrophotometer is briefly introduced, in Sect. 2.2 the GOME2/MetopA GODFIT_v3 algorithm is discussed, in Sect. 2.3 the application of the two effective temperatures on the Dobson TOCs is explained, as well as their comparison to auxiliary in situ-derived data. In Sect. 3 the results are analysed and main conclusions follow in Sect. 4.

2 Data and methodology

2.1 The Dobson spectrophotometer total ozone columns

The Dobson instrument is a double monochromator with a dispersing spectrometer and a recombining spectrometer (Dobson, 1957a, b). Consisting of a double prism monochromator, it is designed to measure the differential absorption in the ultraviolet (UV) region where O_3 absorbs strongly. Thus, the difference of intensities of the wavelengths, and not the absolute intensities of the single wavelengths, is measured by Dobson spectrophotometers. A discussion of the different error sources for the total ozone measurements with the Dobson instrument is given by Basher (1982), who concludes that with a well-calibrated Dobson instrument, the error on individual total ozone measurements may be estimated to be 2–3 %, later updated in Staehelin et al. (2003).

A continuously updated selection of the Dobson instruments reporting data to the World Ozone and Ultraviolet Data Centre (WOUDC) at Toronto, Canada, has already been used in the validation of different satellite TOC products such as in the works of Balis et al. (2007b), Antón et al. (2009), Loyola et al. (2011), Koukouli et al. (2012), Labow et al. (2013), Bak et al. (2015) among others. The station selection investigation and criteria have been explained in detail in Balis et al. (2007a, b) and, naturally, a continuous update of the in-house quality assurance of the chosen WOUDC stations is performed annually.

In this study, direct sun daily mean TOC values reported by 53 Dobson stations around the globe have been used as the validation standard; 19 of those are located in the Southern Hemisphere and 34 in the Northern Hemisphere. Out of these stations, seven also host a Brewer spectrophotometer. The intercomparison between the TOCs reported by a Brewer and a Dobson instrument located in the same site often proves to be a useful tool as there is a seasonality in the Brewer–Dobson differences to satellites investigated also in the past (see Fig. 1, as well as de Backer and De Muer, 1991; van Roozendael et al., 1998; Vanicek, 2006; Scarnato et al., 2010). These comparisons can prove to be a useful tool when assessing the temperature dependence of the Dobson absorption coefficients, since the Brewer wavelengths were chosen so that stratospheric temperature changes would have the least effect on their reported TOCs (Kerr, 2002). Note that the temperature dependence leads to a reduction in absorption at colder than standard temperatures hence an increase in the observed ozone abundance. The Dobson network however uses even larger absorption coefficients; thus the observed Dobson ozone values are in turn lower which causes, at least partly, the annual pattern in the Dobson–Brewer difference (see Fig. 1 and its discussion in the next section).

Both Brewer and Dobson spectrophotometers employ the ozone absorption cross sections from Bass and Paur (1985a), hereafter BP, for a fixed temperature of -45 and $-46.3\,^{\circ}\mathrm{C}$ respectively, without accounting for their temperature dependence (Bass and Paur, 1985b). Newer spectroscopic data sets have been published (e.g. Serdyuchenko, et al., 2014; Gorshelev et al., 2014), covering a larger spectral range. The Absorption Cross Sections of Ozone (ACSO) committee was established in spring 2009 as a joint ad hoc commission of the Scientific Advisory Group (SAG) of the Global Atmosphere Watch (GAW) of the WMO and the International Ozone Commission (IO3C) of the International Association of Meteorology and Atmospheric Sciences (IAMAS; http://igaco-o3.fmi.fi/ACSO/index.html), to examine the possibility of the harmonization of the ozone cross sec-

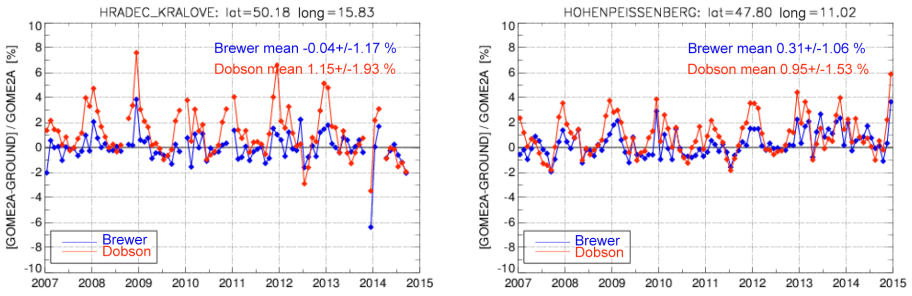

Figure 1. Monthly mean differences between GOME2A and Brewer (blue) and Dobson (red) total ozone columns for two middle-latitude sites, in Hradec Králové, Czech Republic (left panel), and Hohenpeissenberg, Germany (right panel).

tions used in different instruments as well as the temperature dependence of the ozone cross sections and its effect in the ozone retrievals.

For the Brewer spectrophotometer wavelengths, there were many indications that the BP cross section temperature dependence was inconsistent. In particular, the study of Kerr (2002) showed that the temperature dependence of the ozone absorption coefficient at the temperature of $-45\,^{\circ}\mathrm{C}$ was $-0.005\,\%\,^{\circ}\mathrm{C}^{-1}$, revising his previous calculations (Kerr et al., 1988) of $0.07\,\%\,^{\circ}\mathrm{C}^{-1}$. In addition, recent studies (Fragkos et al., 2013; Redondas et al., 2014) estimated the temperature dependence of the ozone absorption coefficient at the temperature of $-45\,^{\circ}\mathrm{C}$ for the Brewer wavelengths based on the set of Serdyuchenko et al. (2014), hereafter Serdyuchenko–Gorshelev or SG data set, in the range 0.009–$0.019\,\%\,^{\circ}\mathrm{C}^{-1}$, very close to the revised value from Kerr (2002) and quite different for those calculated for the BP data set (0.09 and $0.097\,\%\,^{\circ}\mathrm{C}^{-1}$, for Brewers no. 185 and no. 005, respectively). This is a strong indication that the temperature dependence of the ozone cross sections for the Brewer wavelengths is almost negligible. For the Dobson instrument, Redondas et al. (2014), estimated that the temperature dependence of the ozone absorption coefficient is almost identical for both BP and SG data sets (0.133 and $0.104\,\%\,^{\circ}\mathrm{C}^{-1}$ for the temperature of $-46.3\,^{\circ}\mathrm{C}$, respectively), verifying the findings of Komhyr et al. (1993) for the BP cross sections. Thus, even in the case of replacement of the BP ozone cross sections from the SG data set, as suggested by ACSO (WMO/GAW, 2015), there will still be the need for post-corrections of the TOC retrieved by Dobson spectrophotometers.

2.2 The GOME2/MetopA GODFIT_v3 total ozone columns

Within the ESA Ozone-CCI project, total ozone column records from GOME2A have been reprocessed with GODFIT version 3 (Lerot et al., 2014). This algorithm is an evolution of the retrieval baseline implemented in the operational GOME Data Processor v5 (van Roozendael et al., 2012) and is based on the direct fitting of simulated Huggins bands reflectances to the GOME2A observations. As ozone absorption cross sections, the Brion, Daumont and Malicet (BDM) data set was chosen (Daumont et al., 1992; Malicet et al., 1995; Brion et al., 1998) because of its accurate wavelength calibration and high signal-to-noise ratio in the Huggins bands. The GODFIT_v3 data products include a set of auxiliary parameters, among which is the effective temperature, for every satellite pixel in addition to the retrieved total ozone column. This temperature has been computed with the a priori temperature and ozone profiles used to simulate the reflectances. The GODFIT_v3 GOME2A TOCs, as well as those of GOME/ERS2 and SCIAMACHY/Envisat, have been evaluated on a global scale against Brewer and Dobson spectrophotometer TOCs (Koukouli et al., 2015). The mean bias to the ground-based observations is found to be within the $\pm 1\,\%$ level for all three sensors, while the excellent decadal stability of the total ozone columns provided by the three European instruments falls well within the ESA Ozone-CCI project 1–3 % requirement (van der A, 2011).

In Fig. 1 two examples of the validation process shown in Koukouli et al. (2015), are given. The monthly mean differences between GOME2A and ground TOCs are given for the Brewer (blue line) and the Dobson (red line) instruments located in Hradec Králové, Czech Republic (left panel), and Hohenpeissenberg, Germany (right panel). The mean difference and associated 1-sigma standard deviation are also given in the upper right corner. The comparisons are quite good for these two northern middle-latitude stations, with differences well within the $\pm 1\,\%$ level. Since these are coincident measurements in the same location one would expect both types of ground-based instrument to show exactly the same behaviour against the satellite sensor. The larger differences are found for the winter months as expected due to the fact that the effective temperature in the Northern Hemisphere (NH) middle latitudes deviates from $-46.3\,^{\circ}\mathrm{C}$ which is used in the standard Dobson ozone retrieval algorithm. In the following section, the extent of this deviation and the magnitude of how it affects the TOCs is expanded upon.

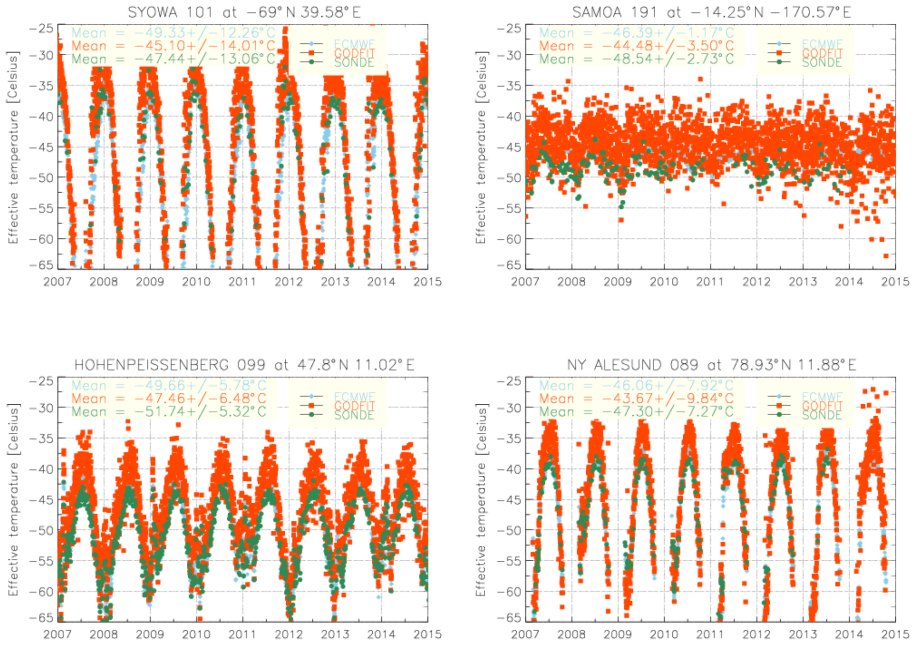

Figure 2. Time series of the effective temperatures estimated by ECMWF (blue), GODFIT_v3 (red) and ozonesondes (green) for four Dobson locations: upper left, an Antarctic station in Syowa; upper right, a tropical station in Samoa; lower left, a northern middle-latitude station in Hohenpeissenberg and lower right, an Arctic station in Ny-Ålesund. The mean values are also given in the upper left corner of each plot.

2.3 The effective temperature dependency

A post-processing of the Dobson TOCs was performed in order to compensate for the well-known effective temperature dependency of the Dobson instruments (Staehelin et al., 2003). In reality, the absorption coefficients depend on temperature; as temperature changes depending on the season and the latitude, the absorption of solar radiation by ozone also changes. Therefore, for an accurate retrieval of TOC the actual temperature at all latitudes and seasons must be taken into account. However, the methodology of TOC retrieval from ground-based measurements does not allow partitioning of the ozone absorption at different atmospheric states. The Dobson instrument algorithm presumes that the stratospheric temperature is equal to −46.3 °C and the Brewer standard algorithm at −45 °C for all latitudes and seasons. Hence, ignoring this effect will lead to a seasonal dependent offset in the total ozone data (Fioletov et al., 2008; van der A et al., 2010).

The effective ozone temperature is defined as the integral over altitude of the ozone-profile-weighted temperature and is derived by

$$T_{\text{eff}} = \frac{\int_0^{\text{top}} T(z)\, \text{O}_3(z) \text{d}z}{\int_0^{\text{top}} \text{O}_3(z) \text{d}z}. \quad (1)$$

Two different effective temperatures were investigated, one provided by the GODFIT_v3 algorithm, as discussed in Sect. 2.2, and one computed from the temperature and ozone profiles provided by a medium-range weather forecasting model by the ECMWF (European Centre for Medium-Range Weather Forecasts; http://www.ecmwf.int/) in order to produce new, post-corrected Dobson total ozone columns and compare them with the satellite TOC measurements. This ECMWF data set was calculated from 6 hourly ECMWF temperature profiles extracted from the operational analyses, and the seasonally dependent Fortuin and Kelder ozone climatology (Fortuin and Kelder, 1998). For each ground station a data set of daily values was created with the effective ozone temperatures interpolated to local noon (van der A et al., 2010).

The behaviour of these two effective temperature data sets was examined using radiosonde and ozonesonde effective temperatures extracted from the WOUDC database as auxiliary data. The criteria by which the selection of the ozonesonde stations was performed are firstly that a collocated Dobson instrument was needed, so as to perform direct comparisons of the effect of the ozonesonde effective temperature with those provided by ECMWF and GODFIT_v3. Secondly, we required global representativeness so as to examine the T_{eff} behaviour of the different data sets at different latitudes. The ozonesonde ozone effective temperature was then calculated using the Eq. (1), with the integration being performed up to the balloon burst height, if that height exceeded the altitude of 30 km. Sondes that burst below 30 km were omitted from the calculations.

In Fig. 2, the effective temperatures are presented as time series for four Dobson locations around the globe: in the upper left plot, the temperatures over the Antarctic station in

Table 1. The details from the four representative Dobson locations presented in Fig. 2 sorted by latitude. The correlations between GODFIT_v3 and ECMWF T_{eff}, as well as between GODFIT_v3 and SONDE T_{eff}, are given in columns six and seven, respectively.

Station name	Location	Latitude	Longitude	Correlation R^2 between GODFIT_T_{eff} & ECMWF_T_{eff}	Correlation R^2 between GODFIT_T_{eff} & SONDE_T_{eff}	Absolute difference between GODFIT_T_{eff} & ECMWF_T_{eff} in °C	Absolute difference between GODFIT_T_{eff} & SONDE_T_{eff} in °C	Number of coincidences
Ny-Ålesund	Norway	78.93	11.88	0.967	0.955	−2.88±1.97	−2.69±2.34	1774
Hohenpeissenberg	Germany	47.8	11.02	0.971	0.952	−1.70±1.40	−0.27±1.75	2550
Samoa	USA	−14.25	−170.57	0.543	0.490	−1.21±1.63	0.39±1.92	1752
Syowa	Antarctica	−69.00	39.58	0.891	0.962	−0.11±4.02	−0.10±2.55	160.3

Syowa are shown; in the upper right plot, the tropical station in Samoa; in the lower left plot, a northern middle-latitude station in Hohenpeissenberg and in the lower right plot, an Arctic station in Ny-Ålesund. The ECMWF effective temperature is shown in blue, the GODFIT_v3 in red and the ozonesonde in green. All three methods seem to depict the seasonal variability quite satisfactorily and the slight bias between the ECMWF and the GODFIT_v3 T_{eff}s in the high northern latitudes (lower right) is not worrisome. The mean values are also given in the figure, where the high standard deviation in the high-latitude stations points to the seasonal variability of the atmospheric state in these latitudes. The correlation coefficients between GODFIT_v3 T_{eff} and ECMWF T_{eff}, as well as those between GODFIT_v3 and SONDE, are given in Table 1, where the details of the four representative Dobson locations are also shown. A very high correlation is found for the high and middle latitudes for both cases. The low correlation for the tropical case (Fig. 2, upper right) may be due to the very small seasonal variability, testified by the low standard deviation of only around 2 °C. As a result, small variations between the T_{eff}s may cause these discrepancies, even though the mean values agree quite well. Additionally, exactly because the effective temperatures in the tropics is very close to the one actually used in the Dobson algorithm, we do not expect those latitudes to be such an issue. The same behaviour was seen in other Dobson tropical stations examined as well (not shown here).

A possible discrepancy in these comparisons may be due to the fact that we used only balloons that burst above the height of 30 km (∼ 10 hPa). No extrapolation method was used to account for the effect of the temperature from the balloon burst height up to the top of the atmosphere, and this may introduce a bias in the retrieved ozone effective temperature. To evaluate this bias we used the daytime v4.2 ozone and temperature profiles from the Microwave Limb Sounder (MLS) aboard the NASA's Aura spacecraft (Waters et al., 2006; Livesey et al., 2008), obtained from NASA's MIRADOR web database (http://mirador.gsfc.nasa.gov/). The useful pressure range for scientific applications for O_3 is from 261 to about 0.02 hPa and for temperature from 261 to 0.001 hPa. Prior to the calculation of the ozone effective temperature, all data quality criteria/flags were used as described in the Data Quality Document (Livesey et al., 2015). In order to firstly demonstrate that the ozone effective temperature calculated by the MLS and the ozonesonde measurements are in agreement, an ozone effective temperature from the altitude range 261–10 hPa was calculated. In Fig. 3, the time series of the two effective temperatures is shown, in the same format as Fig. 2. The agreement for all four locations is spectacular, with a mean difference between ozonesondes and MLS data at a very stable $1.10 \pm 1.00°$. We hence feel confident that the MLS data may act as a proxy for the investigation of the upper stratospheric contribution to the ozone effective temperature, missing from the ozonesonde data. We hence calculated the ozone effective temperature from MLS for the whole pressure range (261–0.02 hPa) and for the layer 261–10 hPa. The difference between the two obtained effective temperatures provided an estimation of the bias of the ozone effective temperature due the fact of limited altitude of the ozonesonde. This bias was found to be $-4.2 \pm 3.27°$ for 3190 coincidences for the Syowa station, $-5.3 \pm 0.60°$ for 3190 coincidences for the Samoa station, $-3.5 \pm 1.22°$ for 2963 coincidences for the Hohenpeissenberg station and $-1.9 \pm 1.45°$ for 3190 coincidences for the Ny-Ålesund station. Considering the differences in latitude, and hence tropopause altitude, of the stations shown, the agreement on the missing upper stratospheric contribution appears to be very stable on a global scale.

We hence feel confident that using the GODFIT_v3-calculated T_{eff}s, even though these are output from the same algorithm that produces the satellite TOCs, will not add any systematic bias in the comparisons with the ground-based TOCs.

3 Results and discussion

In order to post-process the Dobson total ozone columns, Eq. (2) was applied so as to calculate a new total ozone column as was introduced by Komhyr et al. (1993), and was applied in the works of van Roozendael et al. (1998) and van der A et al. (2010):

$$O_{3\,\text{new}} = O_{3\,\text{standard}} \cdot \left[1 - 0.0013 \cdot \left(T_{\text{eff\_new}} - 226.7\right)\right], \quad (2)$$

where

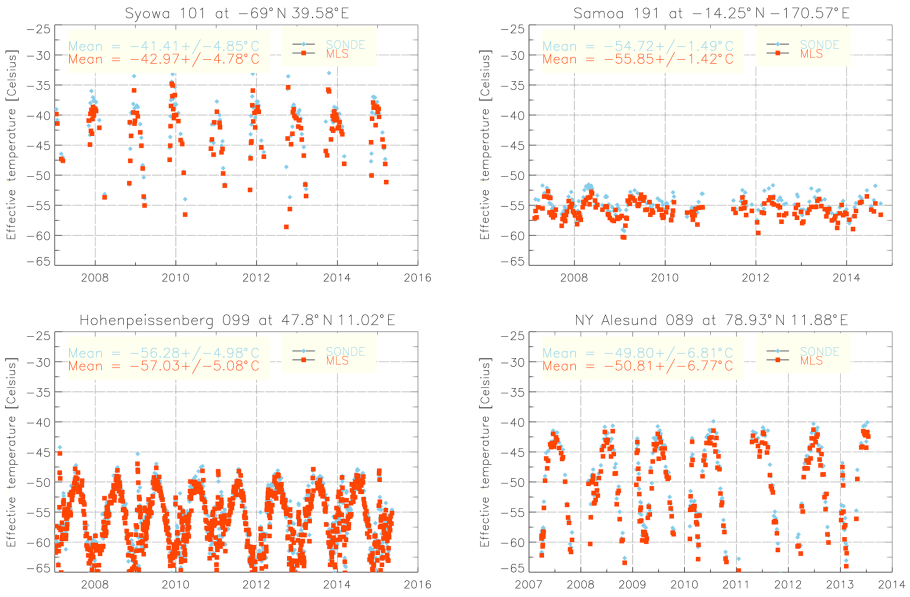

Figure 3. Time series of the effective temperatures between 261 and 10 hPa estimated by the ozonesondes (blue) and the MLS data (red) for the four Dobson locations shown in Fig. 2. The mean values are also given in the upper left corner of each plot.

1. $O_{3\,\mathrm{new}}$ is the new ground total ozone column generated by using the new effective temperature,

2. $O_{3\,\mathrm{standard}}$ is the retrieved total ozone column corresponding to the Dobson reference effective temperature (−46.3 °C),

3. 226.7 is the Dobson reference effective temperature expressed in Kelvin and

4. $T_{\mathrm{eff\_new}}$ is the effective temperatures derived from the GODFIT_v3 algorithm or the ECMWF database.

As a result of Eq. (2), two new post-processed ground-based TOCs exist and their intercomparisons and effect on the original TOC are discussed below in Fig. 4. The comparisons, confined to the Dobson locations, have been averaged into six belts in 30° bins latitude and the following four are shown in Fig. 4 from left to right: the −90 to −60° S belt, the 0 to 30° N belt, the 30 to 60° N belt and the 60 to 90° N belt. In the upper row of Fig. 4, the two temperatures are presented with the GODFIT_v3 shown in orange and the ECMWF in blue. As expected, the higher variability is shown for the Antarctic (first panel) and the Arctic (fourth panel), with temperatures ranging between 200 and 240 K and 220 and 235 K respectively, depending on the season. The NH tropical belt (second panel) shows almost negligible variability, well within 5 K, whereas a 10 K peak-to-peak for the NH middle latitudes (third panel) is found. Note that the Southern Hemisphere (SH) tropical and middle-latitude belts show exactly the same results, in reverse sign, and hence are omitted. As to the actual differences between the two temperatures, for the −90 to −60° S belt it is -0.28 ± 1.16 %; for the 0 to 30° N belt it is very similar at -0.27 ± 0.28 %; for the 30 to 60° N belt at -0.72 ± 0.20 % and for the 60 to 90° N belt, -0.97 ± 0.32 %.

In the lower row of Fig. 4, the effect of post-correcting for the two effective temperatures on the Dobson TOCs is shown for the same latitude bands. The most prominent consequence is found for the Antarctic belt (first panel), with differences in the ozone values ranging from −1 to +3 % depending on the season, followed by the Arctic belt (fourth panel) with differences going from −1 to +1 % or even up to +2 % depending on the year. The effect is not as pronounced for the tropics (second panel) and the middle latitudes (third panel), where the differences go from −0.5 to +1 % for the entire latitude band. The effect of the post-processed Dobson ozone observations on the validation of the GOME2A is given in subsequent figures. To avoid repetitious discussion, only the GODFIT_v3 T_{eff}s will be utilized for the remainder of this paper.

In Fig. 5 the comparisons shown previously in Fig. 1 between the Dobson and Brewer TOCs located in the same station are updated using the post-processed Dobson TOCs, using the GODFIT_v3 effective temperature. The Dobson mean difference to the GOME2A observations has decreased from 1.15 ± 1.93 to 0.29 ± 1.32 % for the Hradec Králové station and from 0.95 ± 1.53 to 0.16 ± 1.08 % for the Hohenpeissenberg Dobson, now bringing the two time series to precisely the same levels.

In Fig. 6 the nominal global validation of the GOME2A GODFIT_v3 data set against collocated Dobson stations is shown in blue and is compared to post-processed Dobson data, in red. Daily percentage differences are either turned

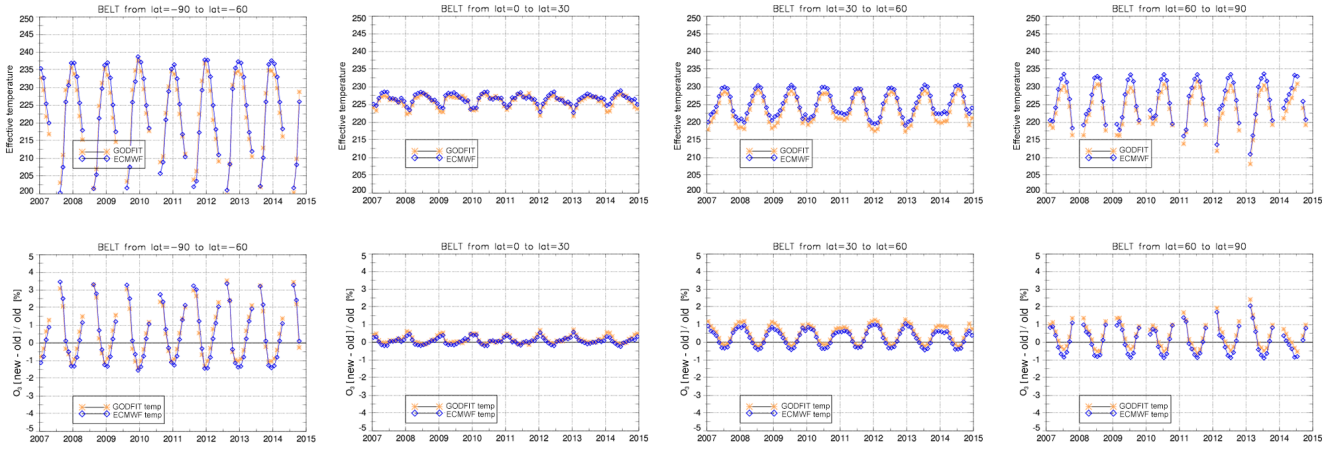

Figure 4. Upper row: monthly mean time series of the effective temperature from the GODFIT_v3 algorithm (orange) and the ECMWF model (blue) for the Dobson locations. Lower row: the percentage difference between the nominal Dobson TOCs and the one calculated using the GODFIT_v3 algorithm (orange) and the ECMWF model (blue) for the Dobson locations. From left to right: the −90 to −60° S belt, the 0 to 30° N belt, the 30 to 60° N belt and the 60 to 90° N belt.

into a month mean (top row), or are averaged in 5° bins for the bottom row comparisons. From the monthly mean percentage differences for the NH (upper left) and the SH (upper right) it is shown that the higher differences between ground and satellite decrease, whereas those monthly means already hovering on the zero line remain unchanged. In numbers, the NH comparisons go from an original 0.63 ± 0.66 to 0.26 ± 0.46 % difference level and the SH comparisons go from 1.25 ± 1.20 to 0.80 ± 0.71 %. Most important is the fact that the solar zenith angle (SZA) dependency issue has been further limited, with the highest deviation decreasing from 2.38 to 1.37 % for the 80–85° bin, and near-zero dependency up to the 60–65° bin (bottom left). The equivalent behaviour of the Brewer comparisons show the same near-zero dependency up to the 60–65° bin and the highest deviation of 2.34 % also for the 80–85° bin (not shown here). However, a one-to-one comparison between Brewer and Dobson results is impossible due to the geographical spread between the two sets of instruments that is quite different.

It should be noted here that this SZA behaviour in the comparisons between satellite and ground-based TOCs has been investigated in numerous validation studies for different satellites instruments and/or algorithms, by e.g. Balis et al. (2007b), Antón et al. (2009) and Koukouli et al. (2012, 2015) among others. It has been shown that the dependency is introduced both in the satellite analysis, as well as in the ground-based instrumentation, e.g. due to an insufficient rejection of stray light into the instrument's field of view at high solar zenith angles. Since the solar zenith angle and effective temperature dependencies are geophysically linked, it has never been possible before in validation studies to separate the two physical effects.

The expected improvement of the differences against the GODFIT_V3 effective temperature is shown in the bottom right panel of Fig. 6 where the dependency has all but disappeared, and difference levels, on a monthly mean scale, remain between 0 and 2 % for almost all temperatures examined. A possible explanation for the remaining differences observed may be the fact that the Dobson TOCs are based on the BP cross section data set, whereas the GODFIT_v3 TOCs are based on the BDM data set. In the study of Fragkos et al. (2013), the effect on the TOCs provided by the Brewer MKII spectrophotometer operating in Thessaloniki, Greece, was investigated using three different sets of ozone absorption cross sections. For daily observations during the decade 2000–2010 it was shown that replacing the BP with the BDM cross sections would introduce a seasonal offset between −2.8 and −4.5 % in the TOCs, while replacing the BP to the SG cross sections would result in a seasonal offset from −0.9 to −0.5%. It is hence not beyond the realm of possibility that the remaining deviations we note in the monthly mean comparisons may be explained by this difference.

Overall, we hence conclude that, on a global scale, satellite–Dobson TOC comparisons benefit from this post-processing of the Dobson TOCs, as long as the T_{eff} employed has been independently validated against an independent source of measurements or modelling results.

4 Conclusions

In this paper, the impact of the total ozone effective temperature on satellite validation using the global Dobson spectrophotometer network was presented using the European Space Agency Ozone Climate Change Initiative GOME-type Direct FITting version 3 algorithm, as it was applied to the GOME2/MetopA observations. Ozone effective temperatures calculated by the GODFIT_v3 algorithm, as well as the ones extracted from the European Centre for Medium-

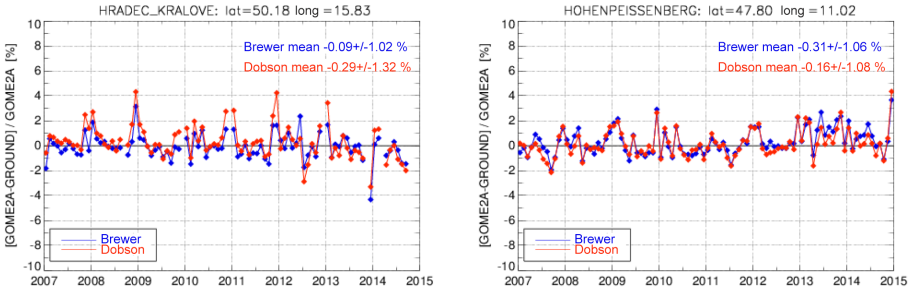

Figure 5. Same as Fig. 1 with the Dobson TOCs being post-processed using the GODFIT_v3 effective temperature.

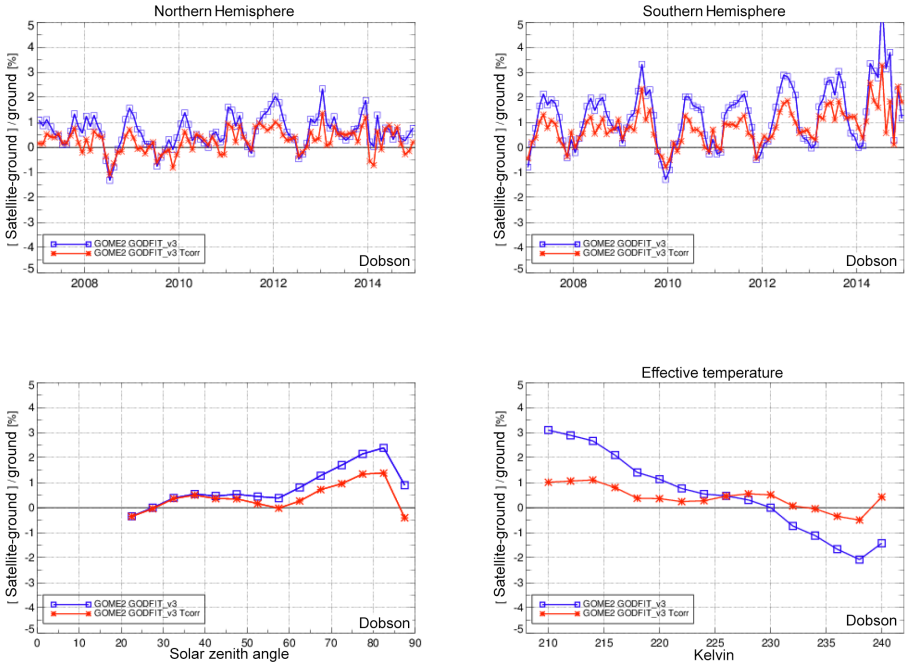

Figure 6. Global comparisons between the nominal (blue) and the post-processed (red) Dobson and GOME2 GODFIT_v3 TOCs. Upper row: the monthly mean time series for the NH (left) and the SH (right) Dobson stations. Bottom row left: the solar zenith angle dependency. Bottom row right: the effective temperature dependency.

Range Weather Forecasts model, were examined and evaluated against collocated ozonesonde measurements. Both sets of effective temperatures were found to agree with the in situ observed effective temperatures to a satisfactory degree and also to result in the same effect on the Dobson total ozone columns. By applying a post-processing to the reported Dobson total ozone columns, the comparisons to the GOME-2A GODFIT_v3 columns results in the following.

1. Examining select stations around the world that host both a Dobson and a Brewer instrument, it was shown that for the Hradec Králové station in the Czech Republic, the Dobson mean difference to the GOME2A observations has decreased from 1.15 ± 1.93 to 0.29 ± 1.32 %, and for the Hohenpeissenberg station, Germany, from 0.95 ± 1.53 to 0.16 ± 1.08 %. The equivalent Brewer statistics are -0.04 ± 1.17 and 0.31 ± 1.06 % respectively.

2. NH comparisons improve from the 0.63 ± 0.66 to the 0.26 ± 0.46 % difference level and the SH comparisons go from 1.25 ± 1.20 to 0.80 ± 0.71 %. Comparisons to Dobson stations located in all latitude bands examined benefit from this post-correction.

3. The solar zenith angle dependency in the satellite-Dobson TOC differences has been reduced with the highest deviation decreasing from 2.38 to 1.37 % for the 80–85° bin, and near-zero dependency up to the 60–65° bin. The equivalent behaviour of the Brewer comparisons shows the same near-zero dependency up to the 60–65° bin and the highest deviation of 2.34 % also for the 80–85° bin.

4. Effective temperatures calculated by either the GODFIT_v3 satellite algorithm or the ECMWF model may be used for the post-processing of the Dobson total ozone columns. This greatly reduces the complex steps to compute ozone effective temperatures from ozonesondes and/or other satellite products.

We hence strongly recommend that any future global satellite total ozone validation activities using the standard Dobson ground-based total ozone measurements be performed using post-processed Dobson total ozone columns using Eq. (2) and quality-assured effective temperature data.

Data availability

i. The ground-based Brewer and Dobson total ozone column data sets presented in this paper originate from the World Ozone and Ultraviolet Radiation Data Centre (WOUDC), one of six World Data Centres which are part of the Global Atmosphere Watch (GAW) and can be found on the official WOUDC pages here: http://woudc.org/data/explore.php.

ii. The GOME2/MetopA GODFIT_v3 Ozone-CCI total ozone column data sets are described in Lerot et al. (2014) and Koukouli et al. (2015) and can be found on the official ESA Ozone CCI pages: http://www.esa-ozone-cci.org/.

iii. The MLS/Aura ozone and temperature profile data sets are described in Livesey et al. (2008) and can be found on the official NASA pages: http://mirador.gsfc.nasa.gov/.

iv. The ozonesonde ozone and temperature profile data sets presented in this paper originate from the World Ozone and Ultraviolet Radiation Data Centre (WOUDC), one of six World Data Centres which are part of the Global Atmosphere Watch (GAW) and can be found on the official WOUDC pages here: http://woudc.org/data/explore.php.

v. The effective temperature data sets presented in this paper originate from the temperature and ozone profiles provided by a medium-range weather forecasting model by the ECMWF (European Centre for Medium-Range Weather Forecasts; http://www.ecmwf.int/) and are described in van der A et al. (2010).

Acknowledgements. The authors would like to warmly thank the scientists working with the Dobson and Brewer spectrophotometers and their continuous efforts to provide timely and quality-assured total ozone columns to the WOUDC database. We would also like to warmly thank the scientists maintaining the WOUDC database for their continuous hard work and immediate response to data requests. The authors would further like to acknowledge the EUMETSAT Satellite Application Facility for Atmospheric Composition and UV Radiation, O3M SAF.

Edited by: M. Weber

References

Antón, M., Loyola, D., López, M., Vilaplana, J. M., Bañón, M., Zimmer, W., and Serrano, A.: Comparison of GOME-2/MetOp total ozone data with Brewer spectroradiometer data over the Iberian Peninsula, Ann. Geophys., 27, 1377-1386, doi:10.5194/angeo-27-1377-2009, 2009.

Bak, J., Liu, X., Kim, J. H., Chance, K., and Haffner, D. P.: Validation of OMI total ozone retrievals from the SAO ozone profile algorithm and three operational algorithms with Brewer measurements, Atmos. Chem. Phys., 15, 667–683, doi:10.5194/acp-15-667-2015, 2015.

Balis, D., Lambert, J.-C., van Roozendael, M., Loyola, D., Spurr, R., Livschitz, Y., Valks, P., Ruppert, T., Gerard, P., Granville, J., and Amiridis, V.: Reprocessing the 10 year GOME/ERS-2 total ozone record for trend analysis: the new GOME Data Processor Version 4.0, Validation,J. Geophys. Res., 112, D07307, doi:10.1029/2005JD006376, 2007a.

Balis, D., Lambert, J. C., van Roozendael, M., Spurr, R., Loyola, D., Livschitz, Y., Valks, P., Amiridis, V., Gerard, P., Granville, J., and Zehner, C.: Ten years of GOME/ERS2 total ozone data: the new GOME Data Processor (GDP) Version 4: I I. Ground-based validation and comparisons with TOMS V7/V8,J. Geophys. Res., 112, D07307, doi:10.1029/2005JD006376, 2007b.

Basher, R. E.: Review of the Dobson spectrophotometer and its accuracy, in: Global Ozone Research and Monitoring Project, no. 13, World Meteorological Organization, Genveva, 1982.

Bass, A. M. and Paur, R. J.: The ultraviolet cross-sections of ozone – I: The measurements: Atmospheric Ozone, Quadrennial Ozone Symposium, Halkidiki, Greece, 3–7 September 1984, edited by: Zerefos, C. S. and Ghazi, A., Springer Netherlands, 1, 606–610, doi:10.1007/978-94-009-5313-0_120, 1985a.

Bass, A. M. and Paur, R. J.: The ultraviolet cross-sections of ozone – II: Results and temperature dependence: Atmospheric Ozone, Quadrennial Ozone Symposium, Halkidiki, Greece, 3–7 September 1984, edited by: Zerefos, C. S. and Ghazi, A., Springer Netherlands, 1, 611–616, doi:10.1007/978-94-009-5313-0_121, 1985b.

Bramstedt, K., Gleason, J., Loyola, D., Thomas, W., Bracher, A., Weber, M., and Burrows, J. P.: Comparison of total ozone from the satellite instruments GOME and TOMS with measurements from the Dobson network 1996–2000, Atmos. Chem. Phys., 3, 1409–1419, doi:10.5194/acp-3-1409-2003, 2003.

Brion, J., Chakir, A., Daumont, D., Malicet, J. and Parisse, C.: High-resolution laboratory absorption cross section of O_3, Tempera-

ture effect, Chem. Phys. Lett., 213, 610–612, doi:10.1016/0009-2614(93)89169-I, 1993.

Brönnimann, S., Staehelin, J., Farmer, S. F. G., Svendby, T., and Svenøe, T.: Total ozone observations prior to the IGY. I: A history, Q. J. Roy. Meteor. Soc., 129, 2797–2817, doi:10.1256/qj.02.118, 2003.

Daumont, D., Brion, J., Charbonnier, J., and Malicet, J.: Ozone UV spectroscopy – I: Absorption cross-sections at room temperature, J. Atmos. Chem., 15, 145–155, doi:10.1007/BF00053756, 1992.

de Backer, H. and De Muer, D.: Intercomparison of total ozone data measured with Dobson and Brewer ozone spectrophotometers at Uccle (Belgium) from January 1984 to March 1991, including zenith sky observations, J. Geophys. Res., 96, 20711–20719, 1991.

Dobson, G. M. B.: Observer's handbook for the ozone spectrophotometer, Ann. Int. Geophys. Year, 5, 46–89, 1957a.

Dobson, G. M. B.: Adjustment and calibration of ozone spectrophotometer, Ann. Int. Geophys. Year, 5, 90–114, 1957b.

Fioletov, V. E.: Ozone climatology, trends, and substances that control ozone, Atmosphere-Ocean, 46, 1, 39–67, doi:10.3137/ao.460103, 2008.

Fioletov, V. E., Kerr, J., Hare, E., Labow, G., and McPeters, R.: An assessment of the world ground-based total ozone network performance from the comparison with satellite data, J. Geophys. Res., 104, 1737–1747, 1999.

Fioletov, V. E., Labow, G., Evans, R., Hare, E. W., Kohler, U., McElroy, C. T., Miyagawa, K., Redondas, A., Savastiouk, V., Shalamyansky, A. M., Staehelin, J., Vanicek, K., and Weber, M.: Performance of the ground-based total ozone network assessed using satellite data, J. Geophys. Res.-Atmos., 113, D14313, doi:10.1029/2008JD009809 2008.

Fortuin, J. P. F. and Kelder, H.: An ozone climatology base on ozonesonde and satellite measurements, J. Geophys. Res., 103, 31709–31734, 1998.

Fragkos, K., Bais, A. F., Balis, D., Meleti, C., and Koukouli, M. E., The effect of three different absorption cross-sections and their temperature dependence on Total Ozone Measured by a Mid-Latitude Brewer Spectrometer, Atmos. Ocean, 53, doi:10.1080/07055900.2013.847816, 2013.

Gorshelev, V., Serdyuchenko, A., Weber, M., Chehade, W., and Burrows, J. P.: High spectral resolution ozone absorption cross-sections – Part 1: Measurements, data analysis and comparison with previous measurements around 293 K, Atmos. Meas. Tech., 7, 609–624, doi:10.5194/amt-7-609-2014, 2014.

Kerr, J.: New methodology for deriving total ozone and other atmospheric variables from Brewer spectrophotometer direct sun spectra, J. Geophys. Res.-Atmos., 107, ACH 22-21–ACH 22-17, 2002.

Kerr, J. B., Asbridge, I. A. and Evans, W. F. J.: Intercomparison of total ozone measured by the Brewer and Dobson spectrophotometers at Toronto, J. Geophys. Res.-Atmos., 93, 2156–2202, doi:10.1029/JD093iD09p11129, 1988.

Komhyr, W., Mateer, C., and Hudson, R.: Effective Bass-Paur 1985 ozone absorption coefficients for use with Dobson ozone spectrophotometers, J. Geophys. Res.-Atmos., 98, 20451–20465, 1993.

Koukouli, M. E., Balis, D. S., Loyola, D., Valks, P., Zimmer, W., Hao, N., Lambert, J.-C., van Roozendael, M., Lerot, C., and Spurr, R. J. D.: Geophysical validation and long-term consistency between GOME-2/MetOp-A total ozone column and measurements from the sensors GOME/ERS-2, SCIAMACHY/ENVISAT and OMI/Aura, Atmos. Meas. Tech., 5, 2169–2181, doi:10.5194/amt-5-2169-2012, 2012.

Koukouli, M. E., Lerot, C., Granville, J., Goutail, F., Lambert, J.-C., Pommereau, J.-P., Balis, D., Zyrichidou, I., van Roozendael, M., Coldewey-Egbers, M., Loyola, D., Labow, G., Frith, S., Spurr, R., and Zehner, C.: Validation of the total ozone climate data record from GOME/ERS, I., SCIAMACHY/Envisat and GOME-2/MetopA as part of the ESA Climate Change Initiative, J. Geophys. Res., 120, 12296–12312, doi:10.1002/2015JD023699, 2015.

Labow, G. J., McPeters, R. D., Bhartia, P. K. and Kramarova, N.: A comparison of 40 years of SBUV measurements of column ozone with data from the Dobson/Brewer network, J. Geophys. Res. Atmos., 118, 7370–7378, doi:10.1002/jgrd.50503, 2013.

Lambert, J.-C., van Roozendael, M., De Mazière, M., Simon, P. C., Pommereau, J.-P., Goutail, F., Sarkissian, A., and Gleason, J. F.: Investigation of pole-to-pole performances of spaceborne atmospheric chemistry sensors with the NDSC, J. Atmos. Sci., 56, 176–193, 1999.

Lambert, J.-C., van Roozendael, M., Simon, P. C., Pommereau, J.-P., Goutail, F., Gleason, J. F., Andersen, S. B., Arlander, D. W., Bui Van, N. A., Claude, H., de La Noë, J., De Mazière, M., Dorokhov, V., Eriksen, P., Green, A., Karlsen Tørnkvist, K., Kåstad Høiskar, B. A., Kyrö, E., Leveau, J., Merienne, M.-F., Milinevsky, G., Roscoe, H. K., Sarkissian, A., Shanklin, J. D., Staehelin, J., Wahlstrøm Tellefsen, C., and Vaughan, G.: Combined characterisation of GOME and TOMS total ozone measurements from space using ground-based observations from the NDSC, Adv. Space Res., 26, 1931–1940, doi:10.1016/S0273-1177(00)00178-2, 2000.

Lerot, C., van Roozendael, M., Spurr, R., Loyola, D., Coldewey-Egbers, M., Kochenova, S., van Gent, J., Koukouli, M., Balis, D., Lambert, J.-C., Granville, J., and Zehner, C.: Homogenized total ozone data records from the European sensors GOME/ERS-2, SCIAMACHY/Envisat, and GOME-2/MetOp-A, J. Geophys. Res.-Atmos., 119, 1639–1662, doi:10.1002/2013JD020831, 2014.

Livesey, N. J., Filipiak, M. J., Froidevaux, L., Read, W. G., Lambert, A., Santee, M. L., Jiang, J. H., Pumphrey, H. C., Waters, J. W., Cofield, R. E., Cuddy, D. T., Daffer, W. H., Drouin, B. J., Fuller, R. A., Jarnot, R. F., Jiang, Y. B., Knosp, B. W., Li, Q. B., Perun, V. S., Schwartz, M. J., Snyder, W. V., Stek, P. C., Thurstans, R. P., Wagner, P. A., Avery, M., Browell, E. V., Cammas, J.-P., Christensen, L. E., Diskin, G. S., Gao, R.-S., Jost, H.-J., Loewenstein, M., Lopez, J. D., Nedelec, P., Osterman, G. B., Sachse, G. W., and Webster, C. R.: Validation of Aura Microwave Limb Sounder O_3 and CO observations in the upper troposphere and lower stratosphere, J. Geophys. Res.-Atmos., 113, D15, 2156–2202, doi:10.1029/2007JD008805, 2008.

Livesey, N. J., Read, W. G., Wagner, P. A., Froidevaux, L., Lambert, A., Manney, G. L., Millán Valle, L. F., Pumphrey, H. C., Santee, M. L., Schwartz, M. J., Wang, S., Fuller, R. A., Jarnot, R. F., Knosp, B. W., and Martinez, E.: Version 4.2x Level 2 data quality and description document, Tech. Rep., Jet Propulsion Laboratory, available at: http://mls.jpl.nasa.gov/data/v4-2_data_quality_document.pdf (last accessed: 30 March 2016), 2011.

Loyola, D. G., Koukouli, M. E., Valks, P., Balis, D. S., Hao, N., van Roozendael, M., Spurr, R. J. D., Zimmer, W., Kiemle, S., Lerot, C., and Lambert, J. C.: The GOME-2 total column ozone product: Retrieval Algorithm and ground-based validation, J. Geophys. Res., 116, D07302, doi:10.1029/2010JD014675, 2011.

Malicet, J., Daumont, D., Charbonnier, J., Parisse, C., Chakir, A., and Brion, J.: Ozone UV Spectroscopy – II: Absorption cross-sections and temperature dependence, J. Atmos. Chem., 21, 263–273, doi:10.1007/BF00696758, 1995.

Redondas, A., Evans, R., Stuebi, R., Köhler, U., and Weber, M.: Evaluation of the use of five laboratory-determined ozone absorption cross sections in Brewer and Dobson retrieval algorithms, Atmos. Chem. Phys., 14, 1635–1648, doi:10.5194/acp-14-1635-2014, 2014.

Scarnato, B., Staehelin, J., Stübi, R., and Schill, H.: Long-term total ozone observations at Arosa (Switzerland) with Dobson and Brewer instruments (1988–2007), J. Geophys. Res., 115, D13306, doi:10.1029/2009JD011908, 2010.

Serdyuchenko, A., Gorshelev, V., Weber, M., Chehade, W., and Burrows, J. P.: High spectral resolution ozone absorption cross-sections – Part 2: Temperature dependence, Atmos. Meas. Tech., 7, 625–636, doi:10.5194/amt-7-625-2014, 2014.

Staehelin, J., Kerr, J., Evans, K., and Vanicek, R.: Comparison Of Total Ozone Measurements of Dobson and Brewer spectrophotometers and Recommended Transfer Functions, WMO TD No. 1147, World Meteorological Organization, Global Atmosphere Watch, No. 149, available at: http://www.wmo.ch/web/arep/reports/gaw149.pdf., 2003.

van der A, R. J.: User Requirement Document, Ozone_cci_URD_2.1, Ozone-CCI, 2011, available at: http://www.esa-ozone-cci.org/?q=webfm_send/37 (last access: 23 December 2015), 2011.

van der A, R. J., Allaart, M. A. F., and Eskes, H. J.: Multi sensor reanalysis of total ozone, Atmos. Chem. Phys., 10, 11277–11294, doi:10.5194/acp-10-11277-2010, 2010.

Vanicek, K.: Differences between ground Dobson, Brewer and satellite TOMS-8, GOME-WFDOAS total ozone observations at Hradec Kralove, Czech, Atmos. Chem. Phys., 6, 5163–5171, doi:10.5194/acp-6-5163-2006, 2006.

van Roozendael, M., Peeters, P., Roscoe, H., De Backer, H., Jones, A., Bartlett, L., Vaughan, G., Goutail, F., Pommereau, J.-P., and Kyro, E.: Validation of ground-based visible measurements of total ozone by comparison with Dobson and Brewer spectrophotometers, J. Atmos. Chem., 29, 55–83, 1998.

van Roozendael, M., Spurr, R., Loyola, D., Lerot, C., Balis, D., Lambert, J.-C., Zimmer, W., van Gent, J., van Geffen, J., Koukouli, M., Granville, J., Doicu, A., Fayt, C., and Zehner, C.: Sixteen years of GOME/ERS-2 total ozone data: The new direct-fitting GOME Data Processor (GDP) version 5 – Algorithm description, J. Geophys. Res-Atmos., doi:10.1029/2011JD016471, 2012.

Waters, J. W., Froidevaux, L., Harwood, R. S., Jarnot, R. F., Pickett, H. M., Read, W. G., Siegel, P. H., Cofield, R. E., Filipiak, M. J., Flower, D. A., Holden, J. R., Lau, G. K., Livesey, N. J., Manney, G. L., Pumphrey, H. C., Santee, M. L., Wu, D. L., Cuddy, D. T., Lay, R. R., Loo, M. S., Perun, V. S., Schwartz, M. J., Stek, P. C., Thurstans, R. P., Boyles, M. A., Chandra, K. M., Chavez, M. C., Chen, G.-S., Chudasama, B. V., Dodge, R., Fuller, R. A., Girard, M. A., Jiang, J. H., Jiang, Y., Knosp, B. W., LaBelle, R. C., Lam, J. C., Lee, K. A., Miller, D., Oswald, J. E., Patel, N. C., Pukala, D. M., Quintero, O., Scaff, D. M., Van Snyder, W., Tope, M. C., Wagner, P. A., and Walch, M. J.: The Earth observing system microwave limb sounder (EOS MLS) on the aura Satellite, IEEE T. Geosci. Remote Sens., 44, 1075–1092, doi:10.1109/TGRS.2006.873771, 2006.

Weber, M., Lamsal, L. N., Coldewey-Egbers, M., Bramstedt, K., and Burrows, J. P.: Pole-to-pole validation of GOME WFDOAS total ozone with groundbased data, Atmos. Chem. Phys., 5, 1341–1355, doi:10.5194/acp-5-1341-2005, 2005.

WMO/GAW: Absorption Cross-Sections of Ozone (ACSO), Status Report, GAW Report No. 218, 2015.